

STRATOSPHERIC MODELLING WITHIN UGAMP

J Thuburn

CGAM, Department of Meteorology, University of Reading,
Reading, United Kingdom

Summary: This paper describes some of the practical problems encountered in adapting a numerical weather prediction model for simulating the climate of the middle atmosphere, and some attempts to solve these problems. These problems include the calculation of water vapour saturation mixing ratios at low pressures, the generation of spurious oscillations in temperature and tracer profiles near the tropopause by the vertical advection scheme, instability associated with the spatial and temporal interpolation of radiative heating rates, and the parameterization of gravity wave drag.

1. INTRODUCTION

The UK Universities Global Atmospheric Modelling Programme (UGAMP) began in 1987. Its purpose is to study the Earth's climate using a range of models. The most sophisticated of these models is based on a version of the ECMWF weather forecast model, adapted and extended in a variety of ways. One extension has been to expand the model domain to include the stratosphere and mesosphere - the resulting model is referred to as the extended UGAMP global circulation model, or EUGCM. The EUGCM is described in section 2.

Development of a complex model is bound to entail difficulties, and the EUGCM is no exception to this. At one extreme, some difficulties are of a superficial, practical nature and are straightforward to fix once the problem has been identified. At the other extreme, some difficulties are of a profound, scientific nature requiring years of research for progress to be made. Section 3 of this paper describes some of the problems encountered in the development of the EUGCM, and the solutions adopted so far, in the hope that the sharing of this experience might be of benefit to other model builders.

2. THE EUGCM

2.1 Model domain and dynamics

The EUGCM (Gray et al. 1993) is an extension of the ECMWF cycle 27 weather forecast model. The dynamical part of the model integrates the hydrostatic primitive equations on a global domain using the spectral transform method (e.g., Hoskins and Simmons 1975). The model has 47 levels extending from the ground to the mesopause and above and uses the hybrid σ - p vertical coordinate and vertical difference scheme of Simmons and Burridge (1981) except for the vertical advection terms (see section 3.2). For most experiments to date, a T21 horizontal resolution has been used. At this resolution a time step of 15

minutes is used and a ∇^8 horizontal scale selective dissipation is applied to the vorticity, divergence, temperature and moisture fields with a damping time scale of 3 hours for the highest resolved wavenumber.

2.2 Parameterized processes

The model includes parameterization schemes to represent boundary layer processes (vertical diffusion), large scale condensation and rain, and some surface processes (Tiedtke et al. 1988). Two different convection schemes are available, a Kuo scheme (Tiedtke et al. 1988) and an adjustment scheme (Betts and Miller 1993).

Two separate radiation schemes are used in the model; in the troposphere and lower stratosphere Morcrette's (1990) scheme is used while at higher levels the schemes of Shine (1987) and Shine and Rickaby (1989) are used. For more details see section 3.3.

The EUGCM also includes the orographic gravity wave drag scheme of Palmer et al (1986). This has been modified to exert a larger fraction of the drag at low levels, following Miller et al (1989), and to include a simplified representation of horizontally travelling non-orographic waves (Jackson 1993). The gravity wave drag scheme is discussed further in section 3.4.

3. SOME DIFFICULTIES ENCOUNTERED IN MODELLING THE STRATOSPHERE

This section describes four of the problems encountered in developing the EUGCM. They range from the almost trivial to the extremely difficult.

3.1 Water vapour saturation mixing ratio

Condensation and evaporation of water are important thermodynamic processes and must be included in a global circulation model. Water vapour mass mixing ratio, q , is a model prognostic variable. The saturation vapour pressure, e_{SAT} , is a function of temperature, T , given by integrating the Clausius-Clapeyron relation. These two quantities, q and e_{SAT} , cannot be compared directly, so either the water vapour partial pressure or the saturation mixing ratio must be calculated. Condensation is assumed to occur when

$$e > e_{SAT}, \quad (\text{EQ 1})$$

where the vapour pressure, e , is given by

$$e = \frac{pq}{(\varepsilon + (1 - \varepsilon)q)}, \quad (\text{EQ 2})$$

p is the pressure and $\varepsilon = R_D/R_V \approx 0.62$ is the ratio of the gas constants for dry air and water vapour, or, equivalently, when

$$q > q_{SAT}, \quad (\text{EQ 3})$$

where

$$q_{SAT} = \frac{\varepsilon e_{SAT}}{(p - (1 - \varepsilon) e_{SAT})}. \quad (\text{EQ 4})$$

In the EUGCM the inequality (3) is used as the criterion for condensation.

A problem arises at low pressures, typically in the lower mesosphere and above, when the denominator in (4) can become negative. Then q_{SAT} becomes negative and (3) is satisfied by any water vapour mixing ratio q that is greater than or equal to zero. In consequence, the model attempts to rain until q equals q_{SAT} , generating negative moisture values and, sometimes, very large heating rates, until it 'blows up'.

There are several ways of viewing the problem. One might argue that vapour pressure is a more fundamental physical quantity than mixing ratio, as far as condensation is concerned, and the comparison (1) should be made instead of (3). Certainly the problem would go away if this were done. Alternatively, one could recognize that, physically, condensation cannot occur for $p < e_{SAT}$ and simply impose this constraint, declaring that (3) and (4) are beyond their range of validity at such low pressures. (Mathematically, (3) is not equivalent to (1) at low pressures; the sense of the inequality should be reversed when the denominator becomes negative.) Thirdly, a practical approach is to switch off irrelevant parameterization schemes, including those involving condensation, above the lower stratosphere. This has the added advantage of reducing the computational expense. Both the second and third of these approaches have been used in the EUGCM.

3.2 Vertical advection

The original version of the EUGCM used a centred difference scheme for calculating the vertical advection terms. It is now well known that many simple difference schemes, particularly those using centred differences, can generate spurious oscillations in the advected field near sharp changes of gradient. The region around the tropopause in the EUGCM is particularly susceptible to such spurious oscillations, especially at high latitudes, because sharp vertical gradients can arise there and because there is little vertical mixing to smooth out any oscillations once they arise. The time scale for the oscillations to arise from a realistic (oscillation-free) initial state is of the order one month, which is the same as the time scale given by the model level spacing divided by the mean vertical velocity in that region.

Firstly, there is a sharp change in the vertical gradient of temperature at the tropopause, so that the centred difference scheme for vertical advection leads to spurious oscillations in temperature. Figure 1 shows an example from an EUGCM integration. Physically, one would expect radiation to damp such temperature oscillations on a time scale less than one month. However, in the example shown, the temperature field was smoothed before being fed into the radiation scheme, preventing the radiation from damping the temperature oscillations. Using unsmoothed temperatures in the radiation calculations disguises the problem by effectively damping the oscillations as they are formed.

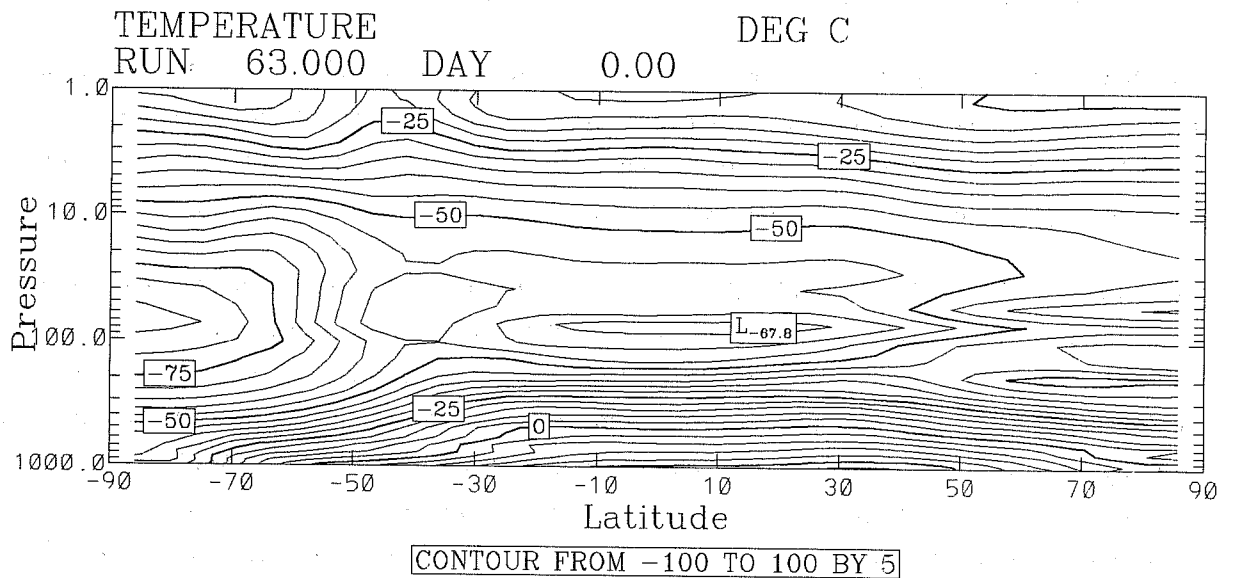


Fig 1. Zonal mean temperature on 15 August from an EUGCM integration using centred differences for vertical advection terms and with vertical smoothing of the temperatures input to the radiation scheme.

Secondly, because the tropopause acts as a barrier to transport, sharp gradients can arise there in the profiles of long lived tracers. Again, the centred difference scheme can generate spurious oscillations, and even negative mixing ratios, (figure 2). In this case the oscillations are not damped by radiation.

Incidentally, a similar problem can arise with non-interpolating semi-Lagrangian advection schemes (as currently used in the ECMWF operational weather forecast model) if the Courant number for vertical advection is small because the scheme then reduces to the basic Eulerian advection scheme.

The solution adopted within UGAMP has been to use flux-limited schemes for vertical advection. Flux-limited schemes ensure conservation by discretizing the flux form of the advection equation,

$$\frac{\partial}{\partial t}(\rho q) + \nabla \cdot (\rho \underline{u} q) = 0, \quad \text{(EQ 5)}$$

while also ensuring some properties implied by the advective form of the advection equation,

$$\frac{Dq}{Dt} = 0, \quad \text{(EQ 6)}$$

namely that no spurious oscillations are produced and existing extrema are not amplified, by carefully constraining or ‘limiting’ the fluxes used in (5). Many different flux-limited schemes are possible. Two have been tried in the EUGCM: one based on second order differences plus the Van Leer limiter (Thuburn 1993), the other based on fourth order differences plus Leonard’s (1991) ‘universal limiter’.

Figure 3 shows the zonal mean temperature from another integration of the EUGCM, in this case using a flux-limited scheme for vertical advection and with no smoothing of the temperature profile seen by the radiation scheme. The spurious oscillations of figure 1 are no longer present. Figure 4 shows the zonal mean distribution of an inert tracer from an experiment analogous to that shown in figure 2 but using a flux-limited scheme for vertical advection. Again, the spurious oscillations are no longer present.

3.3 Radiation - space and time interpolation

Currently the EUGCM uses two radiation schemes: the Morcrette (1990) scheme in the troposphere and lower stratosphere and the schemes of Shine (1987) and Shine and Rickaby (1989) at higher levels. The schemes are merged over a small height range by taking a weighted average of the corresponding heating rates. This merging level can be set by the user and is usually chosen to be between 74hPa and 20hPa.

Ideally, a single radiation scheme should be used through the whole model depth. This would avoid the merging of radiation schemes in the sensitive lower stratosphere where the net heating rate is a small residual of several larger contributions, it would allow the direct communication of radiative fluxes from the troposphere to the stratosphere, and it would reduce the amount of effort required in model development. The first two of these benefits could also be obtained if the merging of the schemes could be made at higher

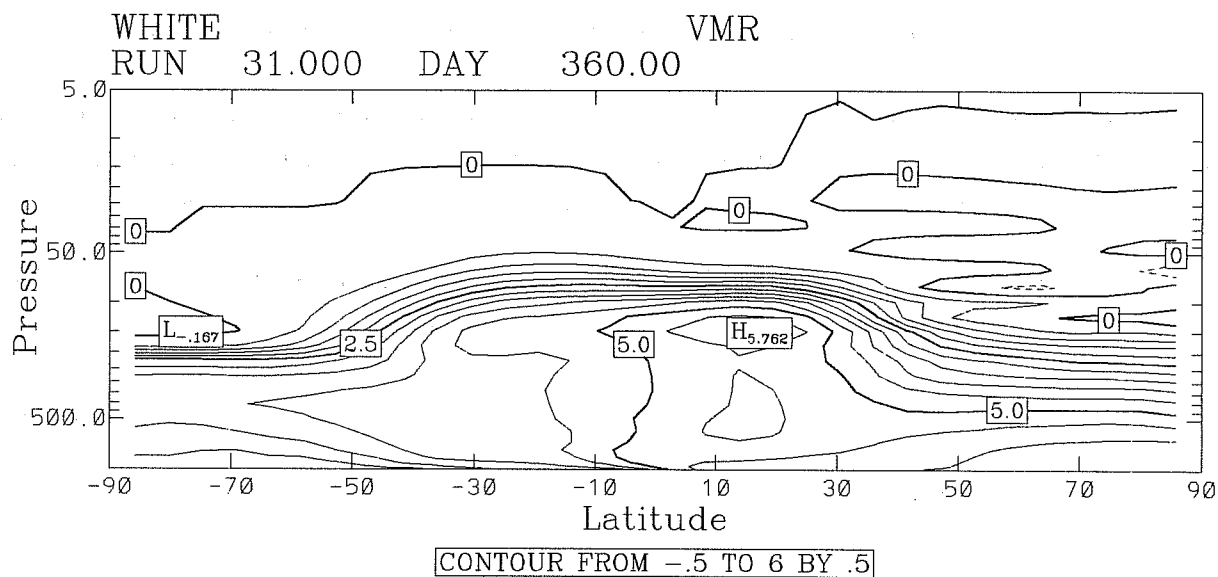


Fig 2. Zonal mean mixing ratio after 360 days of an inert tracer release near the ground in the northern hemisphere. A centred difference vertical advection scheme was used.

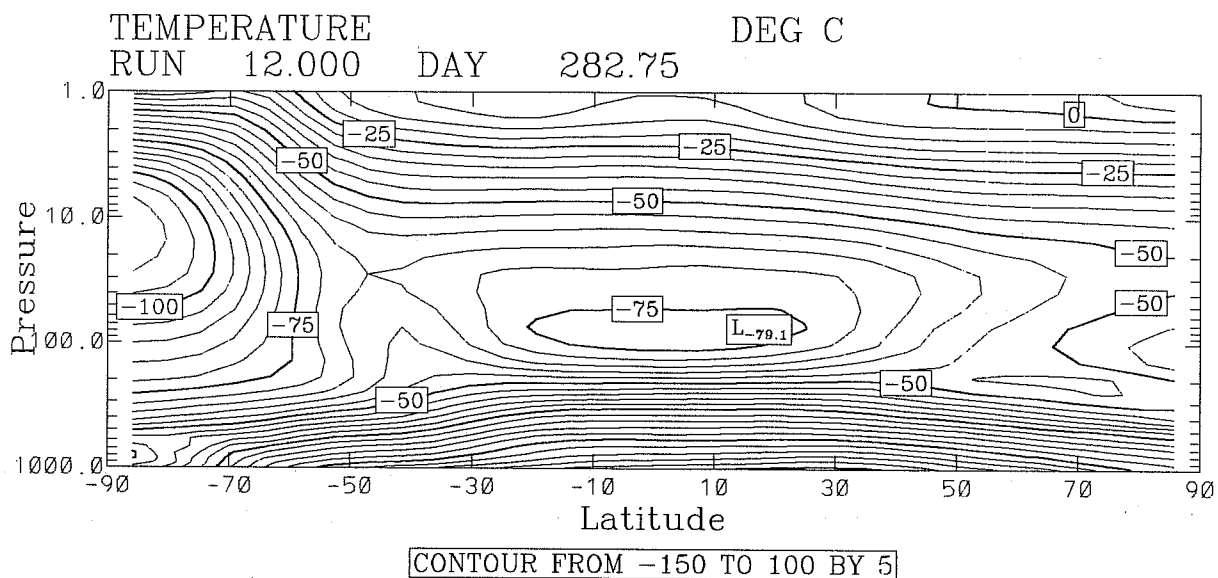


Fig 3. Zonal mean temperature on 15 August from an EUGCM integration using a flux-limited scheme for vertical advection terms and without vertical smoothing of the temperatures input to the radiation scheme.

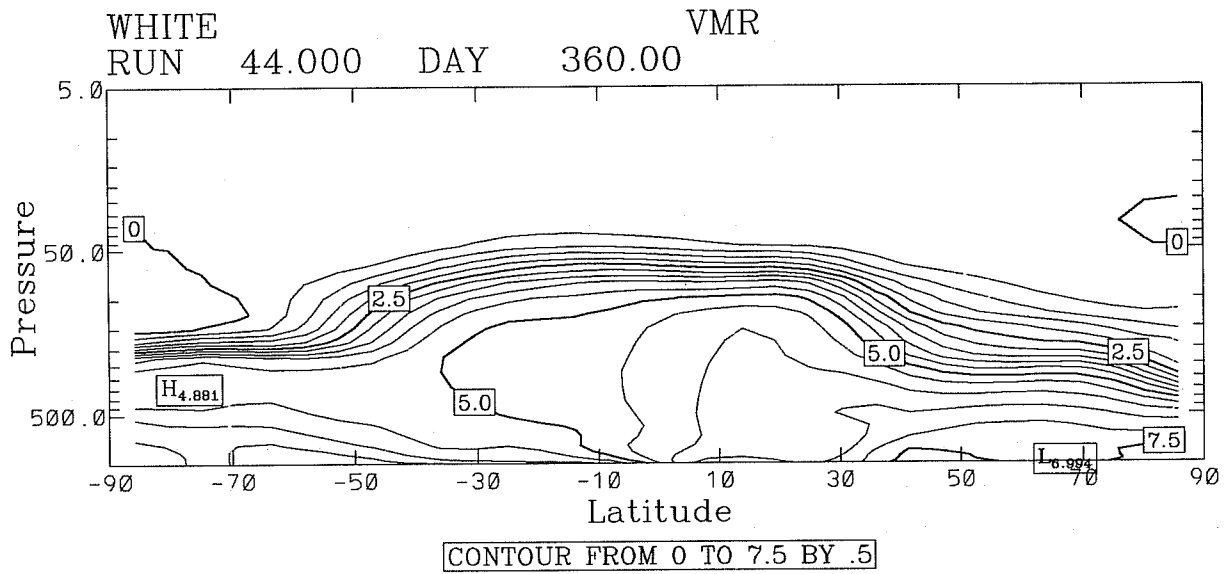


Fig 4. Zonal mean mixing ratio after 360 days of an inert tracer release near the ground in the northern hemisphere. A flux-limited vertical advection scheme was used.

levels. Unfortunately, there is a problem with using the tropospheric radiation scheme at higher levels, associated with the space and time interpolation of the thermal infrared heating.

The Morcrette scheme is computationally expensive, relative to the other components of the model. To reduce the total cost of using the Morcrette scheme in the EUGCM a “full” radiation calculation is made only once every few time steps (typically once every three hours) and then only on a subset of the grid columns (typically every fourth longitude). An attempt is then made to calculate heating rates more cheaply at the intermediate time levels and grid columns, using some information from the full calculation, while taking into account temperature variations (in the long wave) or changes in the Sun’s position (in the short wave). For the long wave part of the tropospheric radiation scheme this is done using “effective emissivities”.

First, the input parameters to the radiation scheme, such as temperature and moisture, are interpolated to the radiation grid using a truncated Fourier series. The full radiation calculation is used to obtain the net long wave irradiance, F_0 , at the boundaries of the model levels. An effective emissivity, ε , is then defined in terms of the irradiance and the local temperature, T_0 ,

$$\varepsilon = \frac{F_0}{\sigma T_0^4}, \quad (\text{EQ 7})$$

where σ is the Stefan-Boltzmann constant. The effective emissivity is extrapolated to other grid columns by fitting a Fourier series and is held constant in time between full radiation calculations. The heating rate at arbitrary longitudes and time steps is calculated by using the local temperature, T , to give the net long wave irradiance, F ,

$$F = \varepsilon \sigma T^4, \quad (\text{EQ 8})$$

and then by taking the vertical derivative of the irradiance. There are three problems with using this method in the stratosphere.

Firstly, it is unphysical. Equation (8) implies that the net long wave irradiance at any level depends on strongly on the temperature at that level. In reality the net long wave irradiance in the stratosphere depends most strongly on conditions far below in the troposphere. In the optically thicker troposphere (8) is a more reasonable approximation.

Secondly, in the stratosphere, the change in the long wave irradiance across one model level is small compared to the irradiance itself. Thus the heating rate is proportional to a small difference of two large terms. Small errors in the irradiance, introduced, for example, by the spatial interpolation, lead to large errors in the heating rate and to a noisy spatial distribution of the heating. Figure 5 shows two examples of heating rate profiles calculated in the EUGCM at a full radiation time step. The solid line is with a full calculation made at every longitude. The dotted line is with a full calculation made every fourth longitude. There are

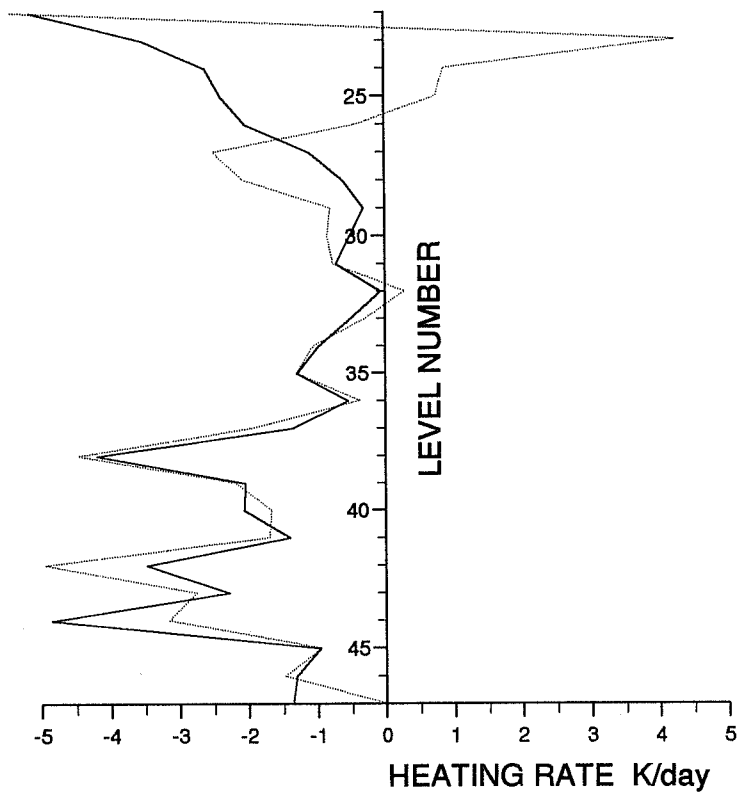


Fig 5. Long wave heating rate as a function of level number calculated for a tropical column of the EUGCM using the Morcrette scheme with the effective emissivity method for spatial interpolation. The solid line is with a full radiation calculation at every longitude; the dotted line is with a full radiation calculation every fourth longitude. The level numbers correspond roughly to the following pressures: level 25, 8.4hPa; level 30, 38hPa; level 35, 190hPa, level 40, 595hPa; level 47, the ground.

differences between the profiles both in the stratosphere and at low levels. The differences in the stratosphere arise for the reason just described. The differences at low levels arise because information is lost interpolating the input parameters to the more coarse grid. For comparison, figure 6 shows heating rates calculated for the same column using what might be called an “effective cooling to space” method; an effective cooling coefficient, α , is defined in terms of the heating rate, \dot{T}_0 , as given by the full radiation calculation, and the temperature, T_0 ,

$$\alpha = -\dot{T}_0/T_0. \quad (\text{EQ 9})$$

The cooling coefficient is interpolated in space and held constant in time, and the heating rate is given by

$$\dot{T} = -\alpha T. \quad (\text{EQ 10})$$

The solid line is identical to that in figure 5. At low levels the dotted line is very similar to the dashed line in figure 5 because the errors there are mainly associated with the interpolation of the fields before input to the radiation scheme. However, in the stratosphere the errors associated with the spatial interpolation of the output of the radiation scheme have almost completely vanished.

Thirdly, the effective emissivity method is unstable in the stratosphere. This may easily be seen as follows. If the temperature, T , differs by a small amount, T' , from the value used in the full radiation calculation, T_0 , then the change to the net long wave irradiance is given approximately by

$$F' \approx 4\varepsilon\sigma T_0^3 T', \quad (\text{EQ 11})$$

and the change to the heating rate is approximately

$$\dot{T}' \approx -\frac{4g\sigma}{c_p} \left(T' \frac{\partial}{\partial p} (\varepsilon T_0^3) + \varepsilon T_0^3 \frac{\partial T'}{\partial p} \right), \quad (\text{EQ 12})$$

where g is the gravitational acceleration and c_p is the specific heat capacity at constant pressure. When the coefficient $\frac{\partial}{\partial p} (\varepsilon T_0^3)$ is less than zero, as it is in the stratosphere where T_0 increases with height, a positive change in the temperature can lead to a positive change in the net heating rate, causing the temperature perturbation to grow.

Figure 7 shows an example of the change in heating rate for a +1K change in temperature at all levels, calculated in three different ways. The solid line shows the change in heating rate given by a full radiation calculation. It is negative at most levels because a warmer atmosphere radiates more. There is a positive peak at low levels where increased emission of radiation by the nearby atmosphere leads to increased absorption by a cloud layer. The heavy dotted line shows the change in heating rate calculated using the effective emissivity method. In the troposphere it is not too different from the full calculation, except that it does not capture the reduced cooling in the cloud layer. (No method that relates heating rates to local temperatures only could capture this effect.) However, in the stratosphere this method gives a net increase

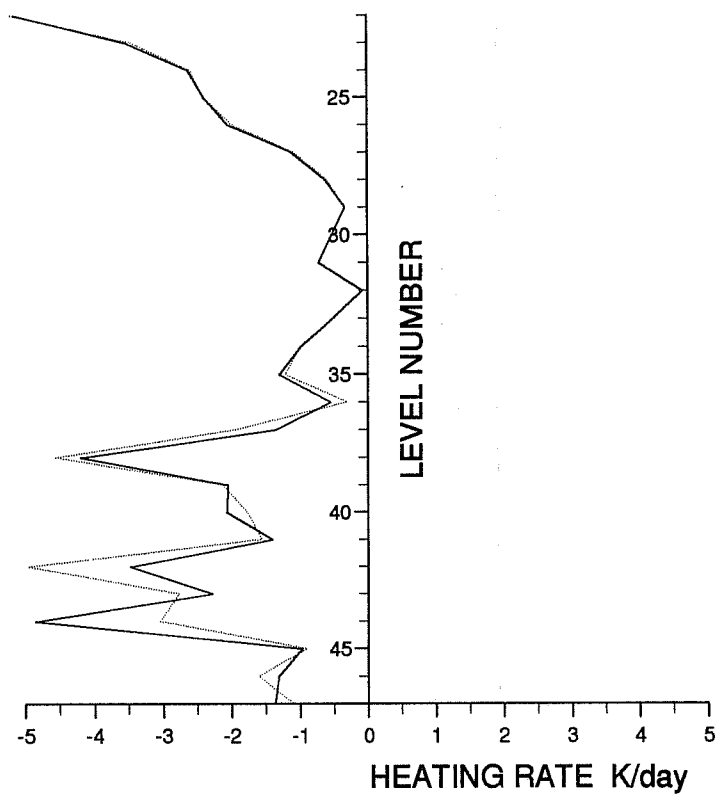


Fig 6. Long wave heating rate as a function of level number calculated for a tropical column of the EUGCM using the Morcrette scheme with the effective cooling to space method for spatial interpolation. The solid line is with a full radiation calculation at every longitude; the dotted line is with a full radiation calculation every fourth longitude.

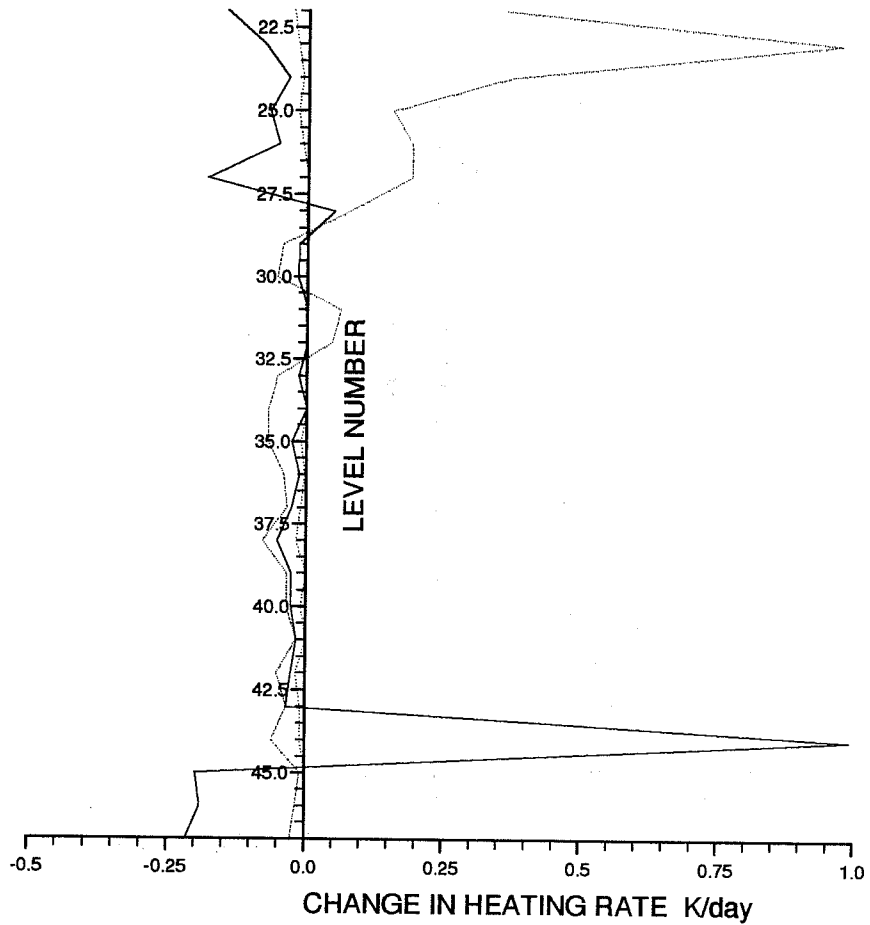


Fig 7. Change in heating rate for a +1K change in temperature at all levels calculated using the full radiation scheme for the original temperature profile followed by (i) using the full radiation scheme on the modified temperature profile (solid line), (ii) using the effective emissivity method on the modified temperature profile (heavy dotted line) and (iii) using the effective cooling to space method on the modified temperature profile (light dotted line).

in the heating of almost 1K/day. This corresponds to an instability with an e-folding time of about 1day. In practice the instability does not usually have time to develop between the three-hourly recalculations of the emissivities, even when the tropospheric radiation scheme is used up to the upper stratosphere. However, in exceptional circumstances, for example, when there is a very strong stratospheric jet, the instability can interact with advected temperature perturbations and cause the model to 'blow up'. The light dotted curve in figure 7 shows the change in heating rate calculated using the effective cooling to space method. Again, this method fails to capture the reduced cooling in the cloud layer. At other levels the change in heating is generally underestimated, though this method is stable.

The solution adopted for the short term in the EUGCM has been to use the middle atmosphere radiation scheme down to the lower stratosphere, despite the drawbacks of this described above. Incidentally, the long wave radiation scheme of Shine (1987) uses a Curtis matrix method. As implemented in the EUGCM, Curtis matrices are calculated at full radiation steps on a subset of the model columns and each matrix is held constant until the next full step and applied over a number of adjacent columns. This method is physically well posed in the middle atmosphere and takes account of changes of temperature (strictly, the Planck function) throughout the column, not just local changes, to calculate the change in heating at any level. It is stable and does not generate spatially noisy heating fields.

The effective emissivity method was compared with an effective cooling to space method in figures 5, 6 and 7. This latter method greatly underestimates the temperature dependence of the heating rate and so is not much better than directly interpolating the heating rates in longitude and keeping them constant in time. However, an improvement on this method would be to express the heating rate as

$$\dot{T} = \beta - \gamma T^4 \quad \text{(EQ 13)}$$

and extrapolate β and γ in space and keep them constant in time. Physically, the γT^4 term represents the emission from the layer in question and the β term represents absorption of radiation emitted by other layers. Thus this is rather like a cheap version of the Curtis matrix method where the dependence on temperatures away from the layer in question has been neglected. The quantities β and γ can be obtained from the full radiation calculation. This method should be stable and should not give spatially noisy heating rates, while it should reflect the dependence on the local temperature better than the effective cooling to space method. It has been tested in a rather different context, to aid convergence in a fixed dynamical heating model to calculate radiative forcing of climate change; it reduces the computer time required to achieve this convergence (Keith Shine, personal communication). It is planned to test this method in the EUGCM in the near future.

With a view to the longer term, the question should at least be raised of whether it might be better to build cheaper, possibly less accurate, radiation schemes that can be applied in every grid column of a GCM, rather than more complex schemes that can only be used in practice with inaccurate spatial and temporal interpolation.

3.4 Gravity wave drag parameterization

Drag exerted on the mean winds by breaking gravity waves is believed to be the dominant mechanism (in conjunction with radiation) driving the circulation in the mesosphere, closing the winter westerly and summer easterly jets and leading to departures from radiative equilibrium, with the winter hemisphere warmer than the summer and an extremely cold summer mesopause. Gravity wave drag is less important at lower levels, though it is believed to be significant in the extratropical lower stratosphere in helping to close the tropospheric westerly jets. It may also be important near the tropical stratopause, contributing to the forcing of the semi-annual oscillation, and around the extratropical winter stratopause, helping to drive descent in the polar vortex. Turbulent mixing associated with breaking gravity waves may also be important for the vertical transport of chemical constituents.

The relevant gravity waves have length scales (both horizontal and vertical) too small to be resolved by most GCMs, so their effects must be parameterized. Unfortunately, our ability to parameterize gravity wave effects is far less advanced than our ability to parameterize radiative processes, for example.

The EUGCM includes the orographic gravity wave scheme of Palmer et al. (1986). In each grid column a source amplitude and direction are calculated, dependent on the sub grid-scale orographic variance and the low level static stability and wind velocity, for a monochromatic gravity wave with zero horizontal phase speed. The wave is then assumed to propagate vertically according to linear, WKB theory, and to break when an estimated wave Richardson number becomes less than 0.25 so as to maintain a 'saturation' amplitude. This scheme has been modified in two ways.

Firstly, additional waves with non-zero horizontal phase speeds have been included so as to allow some waves to reach the tropical and summer mesosphere (Jackson 1993) and to qualitatively capture some of the effects of the filtering of the spectrum of gravity waves by the mean winds. Each additional wave is monochromatic and interactions between the different waves are neglected. The source level, amplitude and horizontal phase velocity of each wave is arbitrarily specified; no attempt is made to relate them to specific source mechanisms. A typical configuration is to use 16 additional waves, each with momentum flux $0.5 \times 10^{-4} \text{ Nm}^{-2}$, launched from the lower stratosphere with phase speeds of 10 ms^{-1} and 20 ms^{-1} in 8 different directions.

Secondly, following Miller et al. (1989), a large fraction of the orographic wave drag (typically 70%) is exerted uniformly over the lowest 20% of the atmosphere. Above this level the original algorithm of Palmer et al. is used. The main motivation for using this modification in the EUGCM is that it reduces the amplitude of gravity waves reaching the stratosphere, leading to improvements in the synoptic behaviour of the vortex.

No attempt is made to represent any vertical mixing that may be caused by breaking gravity waves.

Figure 8 shows the zonal mean zonal wind and temperature averaged over 30 days of a perpetual January EUGCM simulation, together with the corresponding fields for January from the CIRA climatology (Fleming et al 1990). It reveals some of the benefits as well as some of the limitations of the current gravity wave drag parameterization.

Both the winter westerly jet and the summer easterly jet eventually close off near the mesopause, with wind reversals above this in both hemispheres. The drag required to achieve this in the model comes from the additional waves with non-zero phase speed, having been selectively filtered by the mean winds during their upward propagation. Consistent with this, the winter mesosphere is warmer than the summer mesosphere, with a particularly cold summer mesopause. However, the wind reversal above the mesopause is rather too strong in the model, the peak of the winter westerly jet occurs somewhat lower than in the climatology, and the summer mesopause is about 20K colder than implied by the observations. All of these things suggest that the gravity wave drag in the model mesosphere is too strong. The zonal mean drag in the model peaks at over $100\text{ms}^{-1}\text{day}^{-1}$ around the winter mesopause and over $300\text{ms}^{-1}\text{day}^{-1}$ around the summer mesopause.

A very sharp shear zone arises in the model extending upwards and polewards above the summer easterly jet. This coincides with the region of strongest gravity wave breaking. A large fraction of the gravity waves break in this region because their intrinsic phase speed is rapidly reduced as they traverse the shear zone. In turn, the drag exerted by the breaking waves helps to maintain the shear zone. This feedback is probably unrealistically strong because of the simple linear model for the wave propagation, neglecting interactions among the spectrum.

Away from the winter pole, the warm stratopause is maintained by absorption of solar radiation by ozone. There is also a warm stratopause over the winter pole, despite the lack of sunlight; it often appears to be a slightly separate structure from the stratopause at other latitudes. This warm winter polar stratopause must be associated with descent and adiabatic heating. In the model this meridional circulation is driven partly by breaking of (resolved) planetary waves and partly by breaking of (parameterized) orographic gravity waves.

Both of the tropospheric westerly jets in the model appear to extend too high, particularly in the southern summer. Consistent with this, the summer polar lower stratosphere is 10K-15K colder than the climatology. Diagnostics of the gravity wave drag in the model (figure 9) show an almost complete absence of drag in the summer lower stratosphere. In the winter lower stratosphere of the model, orographic wave drag typically peaks at around $2\text{ms}^{-1}\text{day}^{-1}$ near the 40hPa level, whereas a lower breaking level, nearer 100hPa, would help produce a more realistic jet structure. The breaking level coincides with a sharp increase in the static stability; this is consistent with the simple theory on which the parameterization is based. However, the model's temperature structure around the tropopause and in the lower stratosphere is

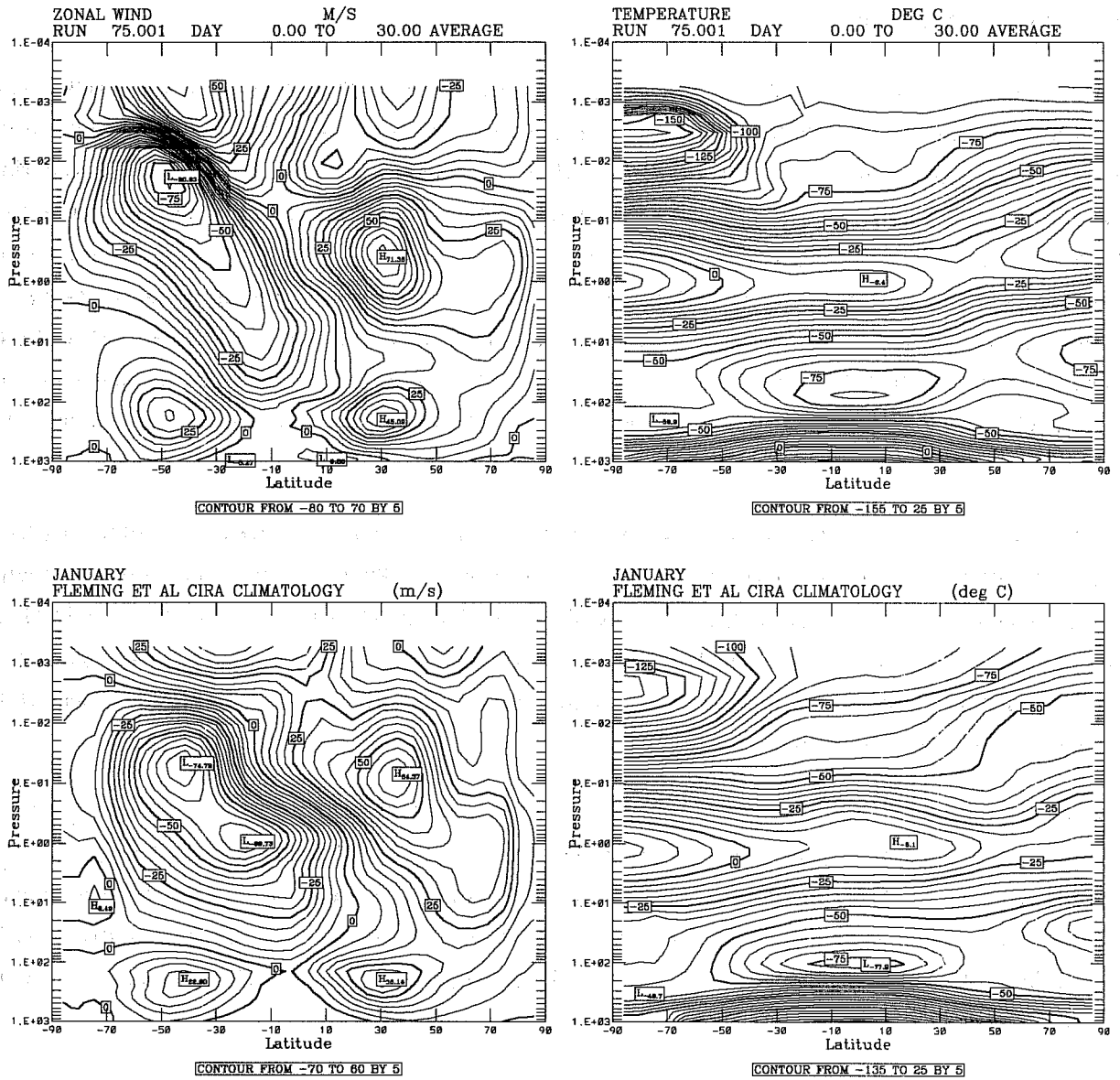


Fig 8. Top left: 30 day mean zonal mean zonal wind from a perpetual January EUGCM integration; top right: 30 day mean zonal mean temperature from the same integration; bottom left zonal mean zonal wind for January from the CIRA (1986) climatology; bottom left: zonal mean temperature from the CIRA (1986) climatology.

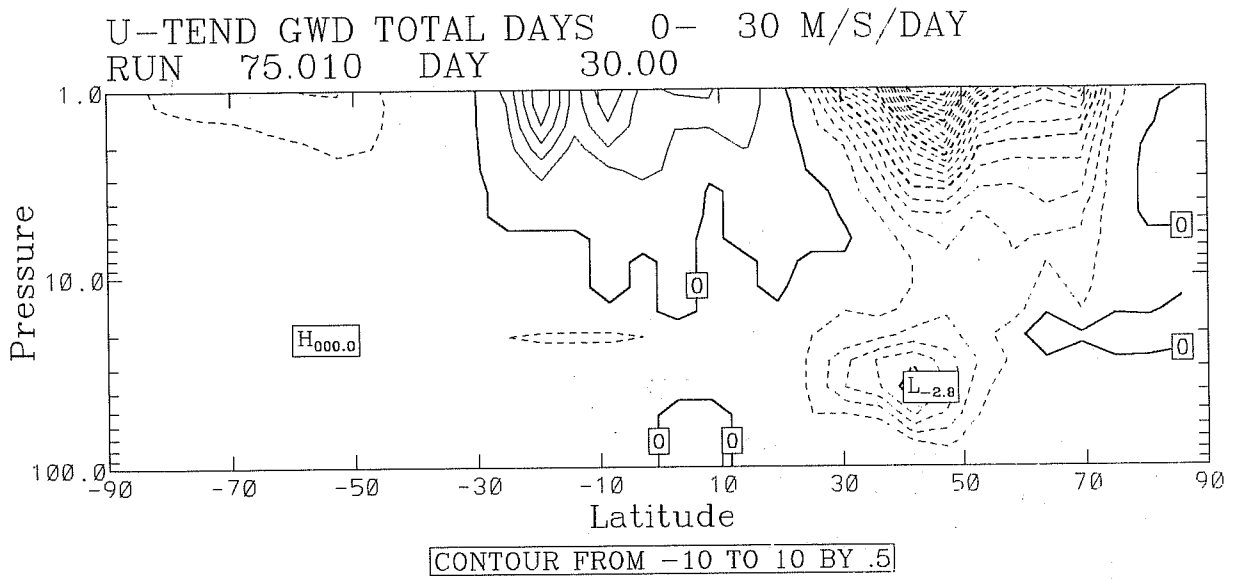


Fig 9. Zonal mean 30 day mean of the zonal wind tendency due to gravity wave drag in the stratosphere from a perpetual January integration of the EUGCM. Contour interval is $0.5\text{ms}^{-1}\text{day}^{-1}$, eastward tendencies are shown by solid contours, westward tendencies are shown by dashed contours.

ERTEL POT VORT
RUN 76.000 DAY

THETA=850.
21.00

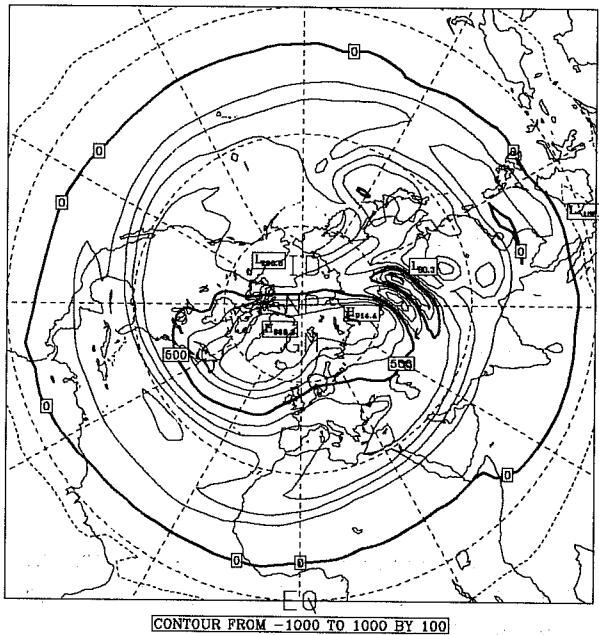


Fig 10. Rossby-Ertel potential vorticity on the 850K isentrope in the northern hemisphere in January from a T42 integration of the EUGCM. Note the unrealistic feature over Asia caused by the gravity wave drag-parameterization.

unrealistic. This, in turn, may be partly caused by the distribution of gravity wave drag, so that it is difficult to determine the origin of the model deficiencies.

While the orographic gravity wave drag appears to be beneficial in maintaining some features of the zonal mean wind and temperature structure, it is detrimental to the synoptic structure of the stratospheric vortex. Strong, localized breaking leads to unrealistic dipole features in potential vorticity maps like that shown over Asia in figure 10 and eventually disrupts the structure of the vortex. The low level drag modification of Miller et al. (1989) helps to reduce this problem at low horizontal resolution (T21). At higher horizontal resolution the problem remains unless an even larger fraction of the drag is exerted at low levels, but this has a detrimental effect on the zonal mean wind and temperature structure, for example, leading to a much weaker winter polar stratopause.

Despite the benefits of the current gravity wave drag scheme, it is not clear that its limitations can be overcome merely by adjusting its tunable parameters. For this reason, two alternative approaches are also being pursued within UGAMP. Firstly, an 'inverse drag' method is being developed for the EUGCM. In this method, the zonal mean winds are relaxed towards their climatological values on an appropriately chosen time scale. As well as forcing the model to simulate a realistic mean state, this method also enables the drag required by the model to achieve that state to be diagnosed. Secondly, a radically different gravity wave scheme based on the observed shape of gravity wave spectra (Fritts and VanZandt 1993, Fritts and Lu 1993) is being tested.

4. SUMMARY

This paper describes four practical problems that have been met in extending a GCM to include the stratosphere and mesosphere. The problem of the criterion for condensation was solved in a straightforward way. The problem of spurious oscillations in tracer and temperature profiles associated with the centred difference vertical advection scheme has been overcome by using flux-limited schemes for vertical advection. A problem has been identified with the use of effective emissivities for interpolating long wave radiative heating rates in space and time. An alternative method has been proposed and is currently being tested. Finally, although a little progress has been made, the problem of parameterizing the drag and mixing due to breaking gravity waves in models of the middle atmosphere is likely to remain one of the most difficult and challenging for many years.

5. ACKNOWLEDGEMENTS

The problem with the criterion for condensation at low pressures was identified by Mike Blackburn. Work on the space and time interpolation of long wave heating rates is being carried out with Keith Shine. Several people are involved or have been involved with developing gravity wave drag parameterizations, including David Jackson, Michael McIntyre, Warwick Norton and Chris Warner.

REFERENCES

- Betts, A K and M J Miller, 1993: The Betts-Miller scheme. In: *The Representation of Cumulus Convection in Numerical Models of the Atmosphere*. Eds K A Emanuel and D J Raymond, American Meteorological Society.
- Fritts, D C and T E VanZandt, 1993: Spectral estimates of gravity wave energy and momentum fluxes. Part I: Energy dissipation, acceleration, and constraints. To appear in *J. Atmos. Sci.*
- Fritts, D C and W Lu, 1993: Spectral estimates of gravity wave energy and momentum fluxes. Part II: Parameterization of wave forcing and variability. To appear in *J. Atmos. Sci.*
- Gray, L J, M Blackburn, M P Chipperfield, J D Haigh, D R Jackson, K P Shine, J Thuburn and W Zhong, 1993: First results from a 3-dimensional model of the middle atmosphere. *Adv. Space Res.*, 13, 363-372.
- Hoskins, B J and A J Simmons, 1975: A multi-level spectral model. I: Formulation and hemispheric integrations. *Mon. Weather Rev.*, 102, 687-701.
- Jackson, D R, 1993: Sensitivity of the extended UGAMP general circulation model to the specification of gravity wave phase speeds. *Q. J. R. Meteorol. Soc.*, 119, 457-468.
- Leonard, B P, 1991: The ULTIMATE conservative difference scheme applied to unsteady one-dimensional advection. *Computer Methods in Applied Mechanics and Engineering*, 88, 17-74.
- Miller, M J, T N Palmer and R Swinbank, 1989: Orographic gravity wave drag: its parameterization and influence in general circulation and numerical weather prediction models. *Meteor. Atmos. Phys.*, 40, 84-109.
- Morcrette, J-J, 1990: Impact of changes to the radiation transfer parameterizations plus cloud optical properties in the ECMWF model. *Mon. Weather Rev.*, 118, 847-873.
- Palmer, T N, G J Shutts and R Swinbank, 1986: Alleviation of a systematic westerly bias in general circulation and numerical weather prediction models through an orographic gravity wave drag parameterization. *Q. J. R. Meteorol. Soc.*, 112, 1001-1039.
- Shine, K P, 1987: The middle atmosphere in the absence of dynamical heat fluxes. *Q. J. R. Meteorol. Soc.*, 113, 603-633.
- Shine, K P and J A Rickaby, 1989: Solar radiative heating due to absorption by ozone. In: *Ozone in the Atmosphere*. Eds R D Bojkov and P Fabian, Deepak Publishing Co., Hampton Virginia.
- Simmons, A J and D M Burridge, 1981: An energy and angular momentum conserving vertical finite difference scheme and hybrid vertical coordinates. *Mon. Weather Rev.*, 109, 758-766.
- Thuburn, J, 1993: Use of a flux-limited scheme for vertical advection in a GCM. *Q. J. R. Meteorol. Soc.*, 119, 469-487.
- Tiedtke, M, W A Heckley and J M Slingo, 1988: Tropical forecasting at ECMWF: The influence of physical parameterization on the mean structure of forecasts and analyses. *Q. J. R. Meteorol. Soc.*, 114, 639-664.